Geotech Geol Eng (2017) 35:1327–1340
DOI 10.1007/s10706-017-0178-z

ORIGINAL PAPER

Shake Table Tests and Numerical Modeling of Liquefaction of Kasai River Sand

Raj Banerjee · Sanku Konai · Aniruddha Sengupta · Kousik Deb

Received: 4 January 2016 / Accepted: 30 January 2017 / Published online: 4 February 2017
© Springer International Publishing Switzerland 2017

Abstract As a part of the seismic safety evaluation of several bridges and other hydraulic structures located on Kasai River bed in India, the liquefaction potential of Kasai River sand is studied in 1-g shake table in laboratory and numerically using a commercial software FLAC 2D. The surface settlement, lateral spreading, predominant frequency, amplification of the ground motion and pore water pressure development in Kasai River sand in dry and liquefied states have been studied when subjected to sinusoidal motions of amplitude 0.35 g at a frequency of 2 Hz. The nonlinear curves used to represent shear strain dependency of stiffness and damping ratio of Kasai River sand are obtained from cyclic triaxial tests. Reasonably good agreement between the experimental and the numerical results is observed. It is found that the settlement and lateral spreading for the liquefied sand is 2.60 and 2.50 times than those of the sand in the dry state. The volumetric strain of the liquefied sand is found to be around 4%, which is significantly higher than 1.53% observed in the dry sand. It is observed that the amplification of the peak ground acceleration for the saturated sand is 1.08 and 1.32 times higher than that for the dry sand from theoretical and experimental results, respectively. The shear strain developed in the liquefied sand is 1.17 times more than that for dry sand. The fundamental and higher modal frequencies of dry sand are found to be 1.13, 1.117 and 1.119 times more than those for the saturated sand, respectively.

Keywords Shake table test · Shear beam analysis · Pore pressure ratio · Liquefaction · Lateral spreading · FLAC 2D

R. Banerjee (✉) · S. Konai · A. Sengupta · K. Deb
Indian Institute of Technology Kharagpur, Kharagpur, India
e-mail: banerjeeraj1990@rediffmail.com

A. Sengupta
e-mail: sengupta@civil.iitkgp.ernet.in

1 Introduction

Liquefaction is one of the most interesting, complex and controversial phenomenon in geotechnical earthquake engineering. The term 'liquefaction' is used in conjunction with a variety of phenomena that involve soil deformations due to cyclic disturbance in a saturated soil under undrained conditions. The generation of excess pore water pressure is the hallmark of all liquefaction related phenomena and the reduction in the volume or the tendency of a cohesionless soil to densify during undrained loading condition as prevails during an earthquake is also well known. The development of pore water pressure starts with the rearrangement of soil grains in loose saturated cohesionless soils when earthquake waves pass through them. The soil grains try to rearrange themselves to take a denser form, and the pore water

pressure increases during this process. The increment in the pore water pressure is directly proportional to the decrement of the effective stresses in a soil. The decrease in grain-to-grain contact or effective stresses causes a decrease in the shear strength of a cohesionless soil and finally leads to the liquefaction or loss of shear strength. The reasons for a liquefaction in a soil are explained by many researchers (Castro 1975; Martin et al. 1975; Ishihara et al. 1975; Seed 1979; Vaid and Chern 1983; Seed et al. 1985; Poulos et al. 1985). The liquefaction response of a soil mainly depends on the initial stress and other state parameters of the soil apart from the ground motion parameters of the seismic shaking (Lee and Seed 1967; Castro and Poulos 1977; Vaid and Finn 1978; Vaid et al. 1985). The liquefaction of soils has been investigated by several researchers using reduced scale models on shake table and centrifuge. Hushmand et al. (1988) and Dobry et al. (1995) carried out centrifuge tests on saturated sand deposits to understand the effect of time histories of accelerations and pore pressures developed during cyclic shaking. The use of shaking table tests to understand the liquefaction of soils has been demonstrated by several researchers (Ye et al. 2013; Ha et al. 2011). Sasaki et al. (1992) carried out shake table tests to understand the ground displacements during liquefaction and concluded that the displacements are due to large shear strains in sand which is softened by the generation of excess pore water pressures. Mohajeri and Towhata (2003) and Towhata et al. (2006) carried out 1-g shaking table tests on soil models prepared in a laminar box to study the rate dependent behavior of liquefied soils. Kokusho (1999) carried out shaking table tests to understand the effect of drainage conditions on the liquefaction-induced deformations. Ueng et al. (2010) used a biaxial laminar shear box mounted on a shaking table to study the settlements in saturated clean deposits of sand and related the volumetric strain in a liquefied sand to the relative density for various shaking durations and earthquake magnitudes. The large scale shaking table tests are also used to understand the behavior of sands under seismic excitations (Thevanayagam et al. 2009; Ecemis 2013). Maheshwari et al. (2012) reported increase in liquefaction resistance of reinforced sand by shaking table tests and concluded that the type and the amount of reinforcement in a soil layer has influence on its liquefaction potential. Toyota et al. (2004) carried out 1-g shaking table tests on Toyoura sand to study the effect of acceleration and frequency on the liquefaction response. These tests are carried out with reduced density to account for the reduced stress levels in 1-g model tests.

The objective of the present study is to compare the behavior of dry and saturated Kasai River sand when subjected to a seismic shaking. The Kasai River separates two growing cities, Medinipur and Kharagpur in the state of West Bengal in India. A number of road and railway bridges exist over the river connecting the two cities. The area being in Seismic Zone III (IS 1893 2002), that is, a zone with moderate probability of earthquake, it is important to characterize the behavior of the Kasai River sand during a possible earthquake event especially when a number of bridges are existing over it. Shake table tests and numerical analyses using a commercial finite difference algorithm called FLAC2D (Itasca 2005) have been utilized to study the difference in behavior of a dry and a liquefied Kasai River sand during dynamic loading conditions.

2 Experimental Setup

The experimental setup consists of a shake table which essentially comprises of a 1 m by 1 m steel table mounted on rails. The load carrying capacity of the table is 5 ton. The table is attached to an actuator which vibrates the table in a uniaxial horizontal direction. The servo hydraulic actuator has a capacity of ±50 kN. It has a stroke length of ±100 mm. The actuator is driven by a controller which has a capability of accepting an actual earthquake (random, cyclic) loading as input and generating it between the frequency range of 0.01 and 50 Hz. The actuator has the capability to hold and restart the loading during a test. It has the facility to increase the base load, frequency and amplitude during a test.

The use of shake table tests in geotechnical engineering offers the advantage of simulating complex systems under controlled laboratory environment and the opportunity to gain insight into the fundamental mechanisms governing the behavior of these systems. The model tests, reported here, are performed in a rigid plexiglass container of dimensions 0.9 m × 0.825 m × 0.858 m (length × breadth × height) with top open. The plexiglass sheets are

16 mm thick and glued to each other as well as fixed in a steel frame consisting of steel angles. All the model tests are conducted in a 1-g environment (Iai 1989). One of the important considerations in laboratory scale dynamic soil performance studies is to replicate the infinite boundary condition in the small test chamber. In an infinitely extended soil layer, the energy associate with the wave propagations diminishes gradually due to the combined effect of hysteretic and radiation damping and also because the energy will spread to a greater volume of soil. In a soil within a test chamber, as in this experimental study, the finite dimension of the soil layer does not allow the complete dissipation of the energy induced by the wave propagation. Moreover the presence of the artificial boundaries induces the generation of P-waves which may add inaccuracies on the expected response. In this study the performance of a soil in a rigid container with absorbing boundaries placed at the ends is investigated. Past studies (Bhattacharya et al. 2011; Lombardi and Bhattacharya 2012), have demonstrated that the presence of foam enables the dissipation of a certain amount of energy. They have also demonstrated that higher absorption may be achieved using thicker sheet of foam.

The mass of the box itself contributes to the inertia effect. Because of the inertia of the box itself, measured acceleration would be less than the actual (Lombardi and Bhattacharya 2012; Elgamal et al. 2003). To account for this effect, a simple correction factor for acceleration given by $(m_1+m_2)/m_1$ is proposed by Lombardi and Bhattacharya (2012). Here, m_1 is the mass of the soil within the container and m_2 is the mass of the test container. In this study, since the mass of the container is significantly less than that for the soil inside the test container, no correction has been applied to the measured accelerations.

The initial case consists of testing the dry sand. In this case, the test container is filled up in stages to a height of 650 mm, with the dry sand at a uniform density of 1600 kg/m^3 (unit weight = 15.7 kN/m^3). Two accelerometers, one near the top and another near the bottom are inserted in the soil in the horizontal direction to measure the amplification of the motions through the sand bed and another accelerometer is placed near the top in the vertical direction to measure the ground settlement during the test. One accelerometer is placed on the shake table itself to double check the motions of the shaking table. All the accelerations are measured at the center of the container, away from the side walls. Thermocol sheets, 16 mm in thickness, are placed on the three inner sides of the plexiglass container to minimize the reflection/refraction of waves from the side walls. It is quite common practice to use thermocol or foam sheets at the boundary walls in a shake table test performed in a rigid box in order to reduce the reflection/refraction of waves from the rigid boundaries. Similar soft material has been already used by others studying dynamic and liquefaction phenomena (Lombardi and Bhattacharya 2012; Giri and Sengupta 2010; Bandyopadhyay et al. 2015; Dash 2010; Ha et al. 2011). A different material called duxseal, has been also considered in the past (Coe et al. 1985), with the aim to reduce the energy and waves reflection/refraction from the end walls of the test chamber. The front plexiglass wall of the container is lightly greased to allow viewing of the behavior of the sand layer during tests.

The liquefaction tests on the sand are carried out on the uniaxial shake table within the same transparent plexiglass container. In a liquefaction test, sample preparation is a major issue because the density and the water content of the sand should be maintained uniform throughout the sand bed. Mullins et al. (1977) described the effect of the sample preparation on sand liquefaction and concluded that the liquefaction response of a soil specimen significantly depends on the method of the sample preparation. A 650 mm high sand bed is prepared inside the test chamber. A pre-calculated amount of water (30.56%) is added to the dry sand to ensure that the degree of saturation of the sand is unity (fully saturated condition) in the test chamber. Three pore water pressure transducers at the middle location of the test chamber and at 11.50, 31.0 and 52.0 from the top surface of the sand bed are utilized to monitor the pore water pressure development in the sand bed during the shaking. These pore water pressure transducers are attached to the walls of the test container. It was not possible to keep the transducers at the centre of the tank for measurements. All the liquefaction tests are conducted with water table maintained at the top surface of the sand bed. All the accelerometers are placed at the same positions as before. As before, 16 mm thick thermocol sheets are placed on three sides of the test chamber to minimize the reflection/refraction of waves at the boundaries. Figure 1 shows the liquefaction test setup for this study.

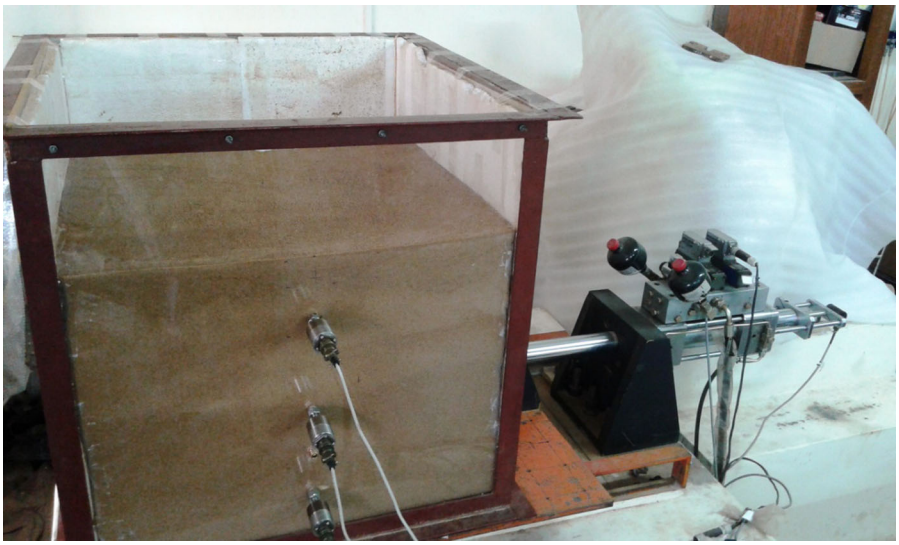

Fig. 1 Test setup for liquefaction

3 Soil Properties

A local uniform grained sand (Kasai River sand) is used in this study. The grain size distribution of the sand as well as the range of gradation for a liquefiable sand given by Xenaki and Athanasopoulos (2003) is shown in Fig. 2. Xenaki and Athanasapoulos (2003) have given the upper and the lower limits of the grain size distribution for liquefaction susceptible soils. The figure indicates that the Kasai River sand is very susceptible to liquefaction as far as the grain size distribution is concerned and hence this study. The Kasai River sand is classified as a poorly graded sand (SP), according to the Unified Soil Classification System (USCS). The specific gravity of the sand is 2.72. The maximum dry unit weight $\gamma_{d(max)}$ is 18.00 kN/m^3, and the minimum dry unit weight $\gamma_{d(min)}$ is 14.00 kN/m^3. The uniformity coefficient (C_u) and the coefficient of curvature (C_c) of the sand are found to be 2.84 and 0.87, respectively. In all the model tests, the bulk unit weight and the relative density (D_r) of the sand are maintained at 15.7 kN/m^3 and 48.7%, respectively. The drained triaxial shear tests are performed on the sand to find its shear strength parameters. The effective cohesion (c') and the effective angle of friction (φ') obtained from triaxial tests are 0.0 kPa and 32°, respectively. The elastic properties of the soil have been found from the initial part of the stress–strain data. Table 1 shows all the material properties for the Kasai River sand. In Table 1, the value of Poisson's ratio is determined by equating the coefficient of earth pressure at rest (K_o) obtained from elastic solution and Jaky's (1944) equation for obtaining K_o value from φ'. The

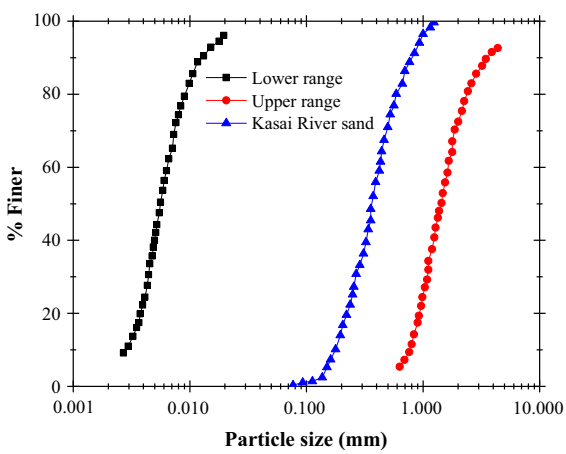

Fig. 2 Liquefaction susceptibility of Kasai River sand

Table 1 Geotechnical parameters of the Kasai River sand

Parameters	Value
Mass density (kg/m^3)	1600
Cohesion (Pa) (c')	0
Angle of internal friction, ϕ'	32°
Modulus of elasticity, E (MPa)	2.938
Poisson's ratio, ν	0.3

liquefaction resistance curve of Kasai River sand is found out from cyclic triaxial tests at 26, 46 and 66 kPa deviator stresses. The tests are conducted on cylindrical specimens (70.84 mm in diameter and 120 mm in height) of the sand. As per ASTM standard D5311 (2011), height-to-diameter (*H/D*) ratio of specimen should be within the range of 2–2.5. However, it has been reported in the literature that the ratio in the range of 1.5–3 does not influence the test results significantly (Ravaska 2006). Thus, the *H/D* ratio of the prepared specimen for the present study is about 1.6 to remain within the stated range. The stress controlled cyclic undrained triaxial tests have been conducted on isotropically consolidated Kasai River sand whose specific gravity is 2.72 and having a relative density of around 50%. The tests have been performed at a loading frequency of 1 Hz for 3 values of critical stress ratio (CSR) of 0.13, 0.23 and 0.33. The variation of the excess pore water pressure ratio, r_u, in the test at different deviator stresses is shown in Fig. 3. The number of cycles needed for liquefaction at different stress level in the Kasai River sand is shown in Fig. 4. It shows that the liquefaction resistance of soil decreases with the increase in the deviator stress. The shear strain level is 1.5% (approx.) at which the soil liquefies. For an illustration purpose, the shear strain time histories for the cyclic triaxial tests conducted at 46 and 66 kPa deviator stresses are shown in Fig. 5. A typical cyclic shear stress vs shear strain curve for a deviator stress of 46 kPa is also shown in Fig. 6.

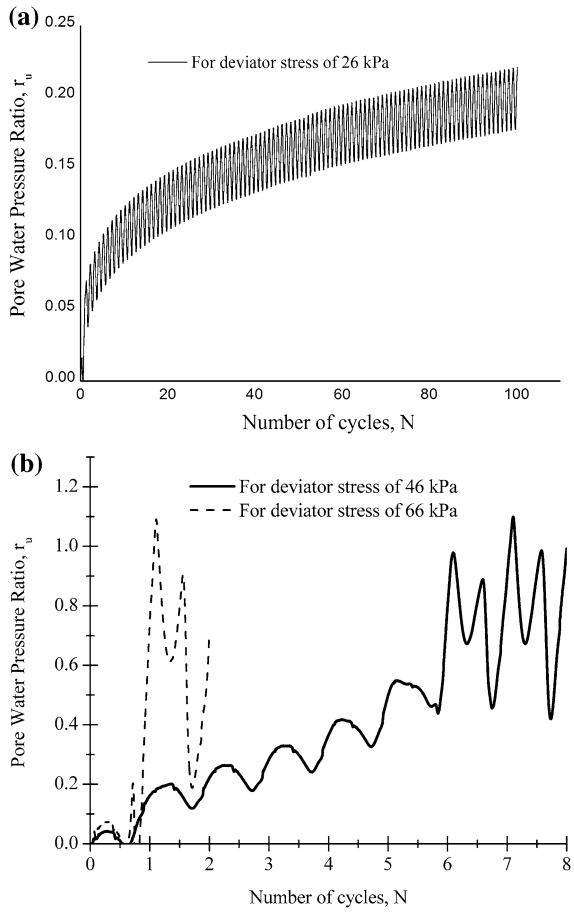

Fig. 3 Variation of pore water pressure ratio, r_u with number of cycles, N for deviator stress of **a** 26 kPa and **b** 46 and 66 kPa in Kasai River sand

4 Selection of Input Motion

The proximity of a number of faults, like Pingla fault, Garhmayna Khandaghosh Fault and Eocene Hinge Zone, to the Kasai River (Dasgupta et al. 2000) has caused mild seismic shaking a number of times in the recent past. A magnitude of $M_w = 4.9$ was recorded at Kharagpur during the 06/02/2008 Earthquake (Raj et al. 2008). The area under consideration comes under the Seismic Zone III in the seismic zonation map of India. The Peak Ground Acceleration (PGA) predicted by GSHAP model (Bhatia et al. 1999) for the area is between 0.2 and 0.3 g. In the present study, the performance of the Kasai River sand is studied conservatively for a 0.35 g event. As a part of the study, a number of earthquake motions are reviewed

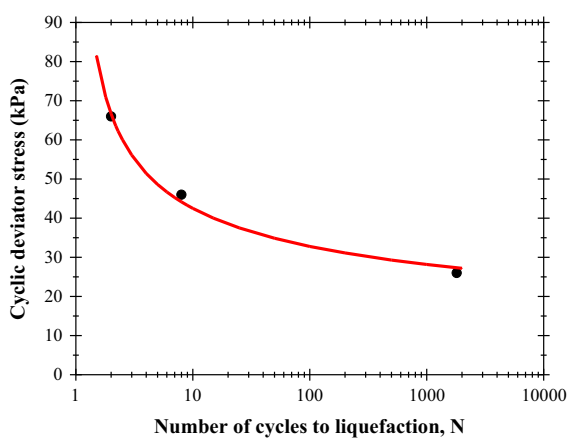

Fig. 4 Cyclic stress needed to produce initial liquefaction

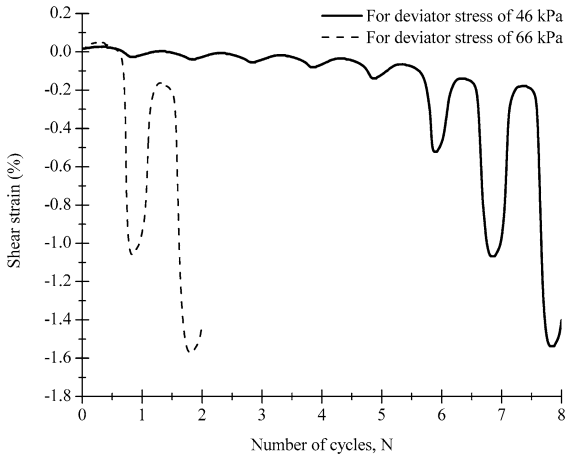

Fig. 5 Variation of shear strain (in %) with number of cycles, N for deviator stress of 46 and 66 kPa

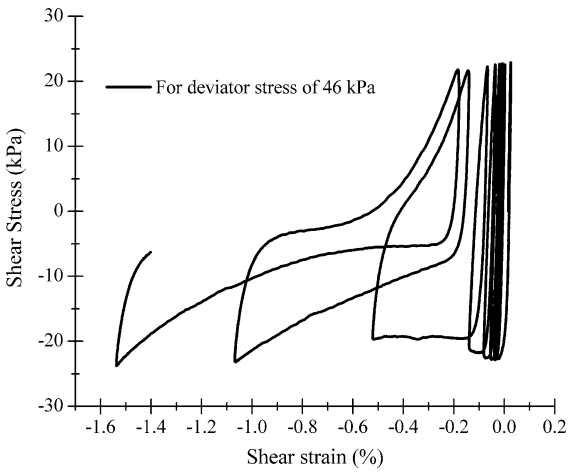

Fig. 6 Variation of cyclic shear stress with shear strain for a deviator stress of 46 kPa

and 03 September, 2010 Darfield Christchurch Earthquake ($M_w = 7.1$, S73 W component) motion is selected for studying the dynamic behavior of the dry and the liquefied sand. The maximum acceleration, *a*, maximum velocity, *v*, maximum displacement, *d*, and predominant period are 490.50, 26.77 cm/s, 10.58 cm, and 0.45 s (2.22 Hz), respectively for the selected motion.

Since dynamic stresses and accelerations are directly related, it is surmised that it is possible to replace the actual acceleration history of Darfield Christchurch Earthquake of $M_w = 7.1$ by a number of cycles of a sinusoidal wave form of constant amplitude in the same manner as it is customary to replace a time history of stresses by a number of cycles of stresses of constant amplitude. Following the procedure developed by Seed and Idriss (1971) to convert an actual irregular stress time history into repetition of several stress cycles of constant amplitude, the equivalent acceleration time history is constructed. The $M_w = 7.1$ earthquake is modeled by 10 cycles of identical full sinusoidal waves. The average value of acceleration amplitude, a_{avg} is calculated as 2/3 of PGA and found to be 0.3503 g with a frequency of 2 Hz. The equivalent acceleration time history selected for studying the dynamic behavior of the dry and the liquefied sand is depicted in Fig. 7. Since the shake table test is done in a small test chamber, the frequency and the duration of the input motions are scaled down by a suitable scaling factor, which is assumed to be 20. Note that the magnitude of the input acceleration is not scaled. The properties of the Kasai River sand, including its density are also not scaled in this study. This is as per the recommendations by Iai (1989) for tests in 1-g environment.

5 Liquefaction Characteristics of the Foundation Soil

The static water level in the sand bed within the test tank is measured before the commencement of the dynamic tests. The pore water pressure at each of the pore pressure sensor locations is recorded to determine the initial static piezometric height. The pore water pressure fluctuations at the specified locations are

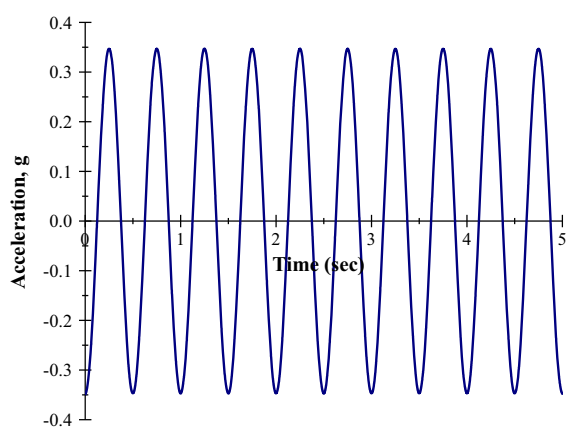

Fig. 7 Equivalent acceleration-time history for liquefaction study

measured during the shake table test and the liquefaction of the sand is assessed. The measurement of the pore water pressure at 0.115 m depth sometimes failed during the test, in which case, the readings of this transducer are not taken into account throughout the study. The variation in the excess pore water pressure, U_{excess} with time at 0.31 and 0.52 m depths within the sand bed is recorded using the remaining two transducers during the test and shown in Fig. 8. The initial effective mean stress (σ_m') at any depth in the soil is used in this study to calculate the pore water pressure ratio (r_u). The value of r_u is defined as the ratio of the excess pore water pressure, U_{excess}, and the initial effective mean stress in the soil at a depth. This is in line with the definition of r_u as defined by Seed and Lee (1966). Seed and Lee (1966) defined the initial liquefaction in a soil as the point at which the increase in the pore water pressure (u_{excess}) is equal to the initial effective all round confining pressure, σ_{3c}'. In the present case, $\gamma_{eff} = 9.28$ kN/m^3, $K_o = (1 - \sin(\varphi)) = 0.47$ and the effective vertical stress at a depth of 0.52 m, $\sigma_z = 4.82$ kN/m^3. Thus the initial effective mean stress at 0.52 m depth, $\sigma_m' = \frac{(1+2K_0)\sigma_v}{3} = 3.12$ kN/m^3. Similarly, the initial effective mean stress at 0.31 m depth is 1.82 kN/m^3. The soil is considered liquefied when r_u is close to 1.0. From Fig. 8, it may be observed that the excess pore water pressures are slightly greater than the mean effective stresses and hence the soil has undergone liquefaction. Note that the initial effective vertical stress at a point is greater than the initial effective mean stress. Thus the pore water pressures developed in the soil are not exceeding the initial effective vertical stress at any point.

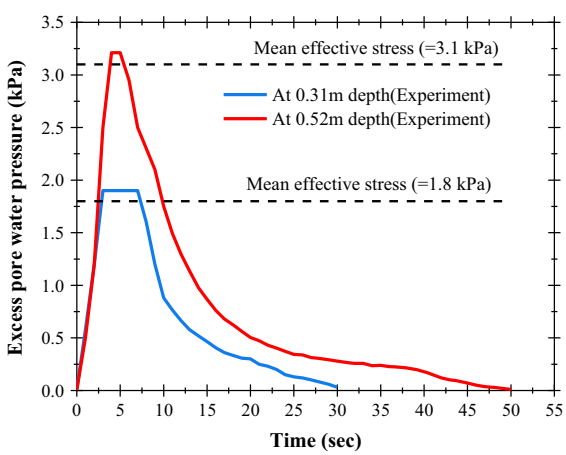

Fig. 8 Variation of excess pore water pressure distributions at various times in the sand

The maximum value of excess pore water pressure, U_{excess} and time elapsed in three different stages of liquefaction (t_1, t_2 and t_3) are evaluated for each transducer and is shown in Table 2. The times t_1, t_2 and t_3 are the time for build-up of liquefaction, duration of liquefaction and the time needed for the dissipation of the excess pore water pressure, respectively.

An important observation made from Fig. 8 is that pore pressure first develops near the top of the sample then proceeds to the middle and eventually to the bottom implying that the sand at shallower depth is more susceptible to liquefaction and therefore, the zone of liquefaction spreads downward from top, a similar observation made by Florin and Ivanov (2006). The time to build up liquefaction for the middle and the bottom transducers is 3 and 4 s, respectively. This supports the above observation. Also, the duration for the liquefaction decreases as we move from top to bottom. This may be observed from Table 2. After the application of about 6–8 cycles (3–4 s) of the sinusoidal motions, the sand liquefies. A number of cracks on the top surface and water gushing out from these cracks are noticeable. It may be noticed from Table 2 that the pore pressure at the mid depth of the sand dissipates faster than that at the bottom of the sand bed. This is attributed to the fact that the drainage for the middle layer is less as compared to the bottom one. Thus, the experimental observations very well match with the theoretical basis, and this validates the experimental results for further study on liquefaction.

6 Seismic Pore Water Pressure Generation Models

The pore pressures and the rate of pore pressure generation with the number of cycles in the Kasai River sand obtained from the shake table tests have been compared with the well established models of Seed et al. (1976) and De Alba et al. (1975). Seed et al. (1976) presented the variation of pore pressure ratio with the number of cycles during the process of liquefaction and showed a typical range for r_u. The pore pressures measured in the present study for the case of the liquefied sand is compared with values given by Seed et al. (1976) in Fig. 9. It is observed that

Table 2 Data from experimental observations

Location of pore pressure transducer	Middle (0.31 m depth)	Bottom (0.52 m depth)
$U_{maximum}$ (kN/m^2)	1.90	3.212
t_1 (sec)	3.0	4.0
t_2 (sec)	4.5	1.5
t_3 (sec)	22.5	44.5

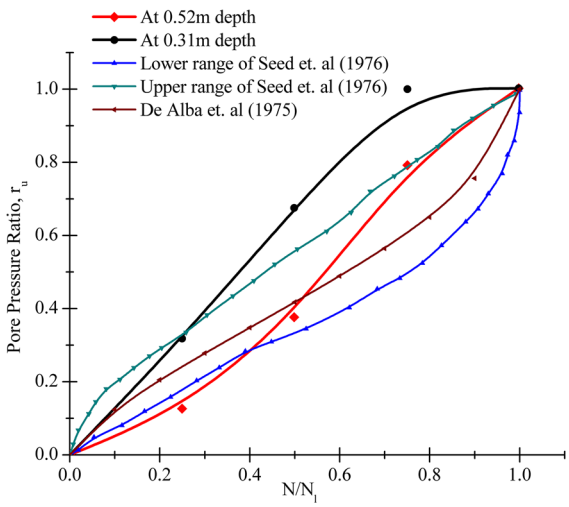

Fig. 9 Rate of pore water pressure generation with normalized number of cycles of load

the rate of pore water pressure generation in the Kasai River sand at a shallower depth (0.31 m) is somewhat higher than the range proposed by Seed et al. (1976). This may be due to a potentially high value of acceleration applied at the base of the shake table. In addition, the sand at a shallower depth (0.31 m) liquefies quickly (at $N/N_l = 0.75$) as compared to the sand at a depth (0.52 m) as illustrated in Fig. 9. In the figure, N represents the number of cycles of loading and N_l represents the number of cycles to liquefaction. De Alba et al. (1975) also presented the rate of pore pressure development with the ratio N/N_l and presented an equation to calculate the pore pressure ratio at any cycle of loading during a liquefaction as:

$$r_u = \frac{1}{2} + \frac{1}{\pi}\sin^{-1}\left[2\left(\frac{N}{N_l}\right)^{1/\alpha} - 1\right] \quad (1)$$

where, N is the number of cycles, N_l is the number of cycles required for liquefaction and α is a coefficient that depends on the soil properties and test conditions, and usually taken as 0.7 for cohesionless soils. Figure 9 also shows the rate of pore water pressure development calculated using the above equation given by De Alba et al. (1975). In the present study, the average value of α for the Kasai River sand is found to be 0.889.

7 Estimation of the Predominant Frequency of Vibration and PGA Amplifications for Dry and Liquefied Sand

In order to have an idea of the shear strain, vibrational frequency and PGA amplification of the Kasai River sand, a theoretical study (uniform shear beam) has been conducted for both dry and liquefied sand. The uniform shear beam procedure is adopted for the Kasai River sand by following an equivalent linear approach that amounts to calculating the dynamic soil properties iteratively until those properties are compatible with the calculated strain level. In order to have an idea of the average deviator stresses that the soil is subjected to, an equivalent linear dynamic analysis have been performed using GEOSTUDIO (QUAKE/W 2004) from which the average cyclic deviator stress is obtained as 66 kPa and 46 kPa for the dry and the liquefied sand. Therefore, the nonlinear material curves used in the shear beam analysis to characterize the dependency of the stiffness of the sand on the strain level are found out by cyclic triaxial tests only for the deviator stresses obtained from the numerical analysis. The dynamic properties (secant shear modulus and damping ratio) of Kasai River sand are mathematically evaluated considering any of the cycles of obtained hysteresis loop for a particular peak shear strain. However, as the tests are done in stress controlled environment in this study, the shear strain varies with each cycle. To account for this asymmetric nature of the hysteresis loops, as shown in Fig. 6, the damping ratio and the shear modulus of the sand have been obtained by a standard procedure proposed by Kreyszig (2010) and Kumar et al. (2015). The nonlinear material curves thus obtained for the Kasai

River sand are compared with the upper range curves for a sand proposed by Seed et al. (1986) and shown in Fig. 10. The results of the shear beam analyses in terms of PGA amplification, predominant periods of the soil and shear strain in the dry and the liquefied state are shown in Tables 3 and 4.

The amplification of a motion is defined as an increase in the seismic ground motion intensity within a soil as compared to that in the underlying firm ground or rock. The above tables indicate that the PGAs on the top of the saturated and the dry sand measured from the shake table tests are comparable with those obtained theoretically. The measured acceleration time histories near the top of the sand in the dry and the saturated condition is shown in Fig. 11. From Fig. 11b, the PGA amplification is found out by taking the ratio of the maximum (absolute) value of accelerations from the top and the bottom time history

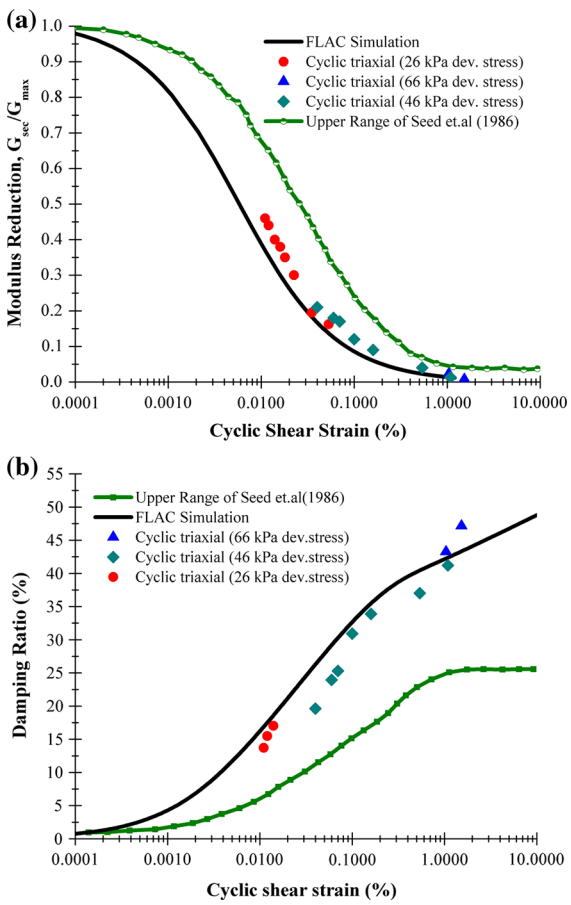

Fig. 10 **a** Degradation of strength and **b** variation of damping ratio with strain in Kasai River sand

Table 3 Uniform shear beam analysis on the saturated sand

Properties	Value
Height of soil column (m)	0.65
Shear strain (%)	10.08
Fundamental frequency (Hz)	0.45
Second modal frequency (Hz)	1.36
Third modal frequency (Hz)	2.26
PGA amplification (Shear beam)	1.30
PGA amplification (Experiment)	1.39

Table 4 Uniform shear beam analysis on the dry sand

Properties	Value
Height of soil column (m)	0.65
Shear strain (%)	8.62
Fundamental frequency (Hz)	0.51
Second modal frequency (Hz)	1.52
Third modal frequency (Hz)	2.53
PGA amplification (Shear beam)	1.20
PGA amplification (Experiment)	1.05

(motions applied at the base of the shake table). This is found to be 1.39 for the liquefied sand. It is observed that the PGA amplification for the saturated sand is around 1.08 and 1.32 times higher than that for the dry sand from the theoretical and the experimental results, respectively. The increase in the amplification of PGA indicates a decrease in the stiffness of the soil column in the liquefied state as compared to that for the dry sand. The decrease in the stiffness is also reflected in the natural frequencies obtained for the dry and the liquefied sand. The fundamental and other modal frequencies of the dry sand are about 1.13, 1.117 and 1.119 times more than that for the saturated sand, respectively. The results obtained from Tables 3 and 4 indicate less damage potential of the structures resting on the dry Kasai River sand as compared to the structures on the liquefied sand.

8 Assessment of Ground Settlement and Lateral Spreading in Dry and Liquefied Sand

The ground settlement and the lateral spreading are major concerns for liquefied soils. For comparison

purpose, the same test with the same amplitude of the sinusoidal motions has been performed on the dry sand also. It is observed that the measured settlement and the lateral spreading are much less in case of the dry sand. Significant settlement and volume changes in the Kasai River sand are observed after liquefaction occurs. For the monitoring of the surface settlements, accelerometers in the vertical direction have been placed on top of the sand layer. The settlement of the sand layer is obtained by integrating the acceleration time history. The ground (surface) settlement time histories during the shake table tests for the dry sand and the liquefied Kasai River sand are shown in Fig. 12a. In this figure, the positive value in the curve indicates heaving and the negative value indicates settlement of the sand. It is observed from the ground settlement curves that the maximum surface settlement in the liquefied sand is almost 26 mm which results in a volumetric strain of 4%, whereas for the dry sand, the maximum observed ground settlement is close to 10 mm which results in a volumetric strain of 1.53%. Thus the ground surface settlement in the liquefied sand is 2.60 times than that for the dry sand under the same dynamic loading condition. After liquefaction, soil samples are collected in thin walled sampler tubes for the measurement of the final density after liquefaction. The initial dry density of the sand is 15.7 kN/m^3 and the final dry density of the liquefied sand is found to be between 16.7 and 17 kN/m^3. Thus the sand densified 1.06 times post liquefaction. The maximum value of the lateral spreading in case of the liquefied sand is also significantly higher (about 2.50 times) as compared to the dry sand as observed from Fig. 12b.

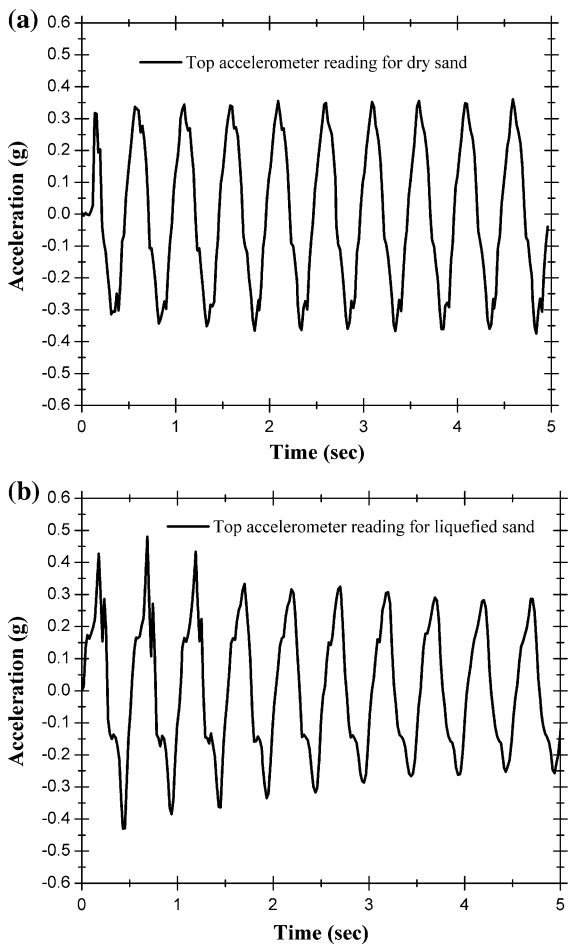

Fig. 11 Acceleration time histories in **a** dry and **b** liquefied conditions of Kasai River sand

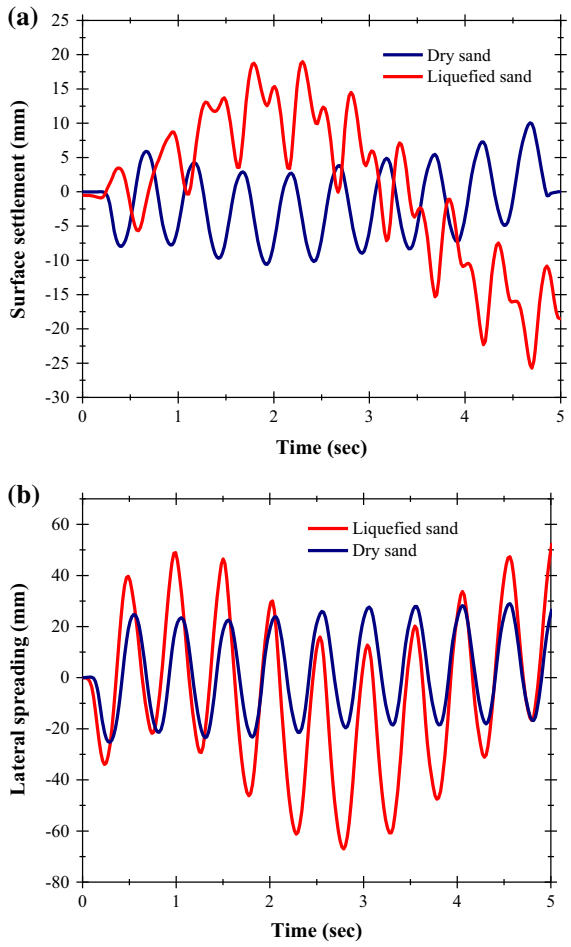

Fig. 12 **a** Surface settlement and **b** lateral spreading time history in dry and liquefied Kasai River sand

9 Numerical Study of Liquefaction

The numerical simulation of the laboratory shake table tests on the Kasai River sand leading to its liquefaction is performed using a commercial finite difference software called FLAC2D. The generation of the pore water pressures in the sand during the dynamic loading is modeled by 'Finn' model. The 'Finn' model is originally developed by Martin et al. (1975) and later modified by Byrne (1991). The FLAC2D incorporates this model in the general Mohr–Coulomb plasticity model to simulate the generation of the pore water pressure during dynamic loading. In this model, the pore water pressure is calculated as:

$$\Delta u = M\Delta\varepsilon_v^p \tag{2}$$

where, Δu = change in pore water pressure, M = constrained modulus of the soil, $\Delta\varepsilon_v^p$ = change in plastic volumetric strain = $\gamma C_1 \exp\left(\frac{-C_2\varepsilon_{vd}}{\gamma}\right)$ with ε_{vd} = change in volumetric strain, C_1 = a constant = $8.7((N_1)_{60})^{-1.25}$, C_2 = a constant = $\frac{0.4}{C_1}$, $(N_1)_{60}$ = normalized SPT values = 8.0 (in the present case) and γ = engineering shear strain.

The locations of the side and bottom boundaries in the numerical analyses are chosen to satisfy the shake table test setup. The numerical analysis is performed after scaling up the dimensions, frequency and the duration of the input motions by the scaling factor 20 assumed before. The results obtained from the numerical analysis are then scaled down by 20 and compared with the corresponding shake table results. The sand bed (17 m in width and 13 m in height) is discretized by 34 × 26 numbers of quadrilateral elements of size 0.5 m × 0.5 m as shown in Fig. 13. The zone (element) size is chosen in a manner such that it is small enough to allow the acceleration waves at the input frequency to propagate accurately (Itasca 2005). The plexiglass test chamber, within which the laboratory shake table tests are conducted, is not modeled in the numerical analyses. In the dynamic analyses, the absorbing boundaries are assumed on the sides. The acceleration-time history given in Fig. 7 and applied to the shake table is assumed to be acting at the bottom of the soil domain. The hysteretic damping and the shakes down of the strength in the Kasai River sand during the dynamic loading are obtained from the cyclic triaxial tests. These two

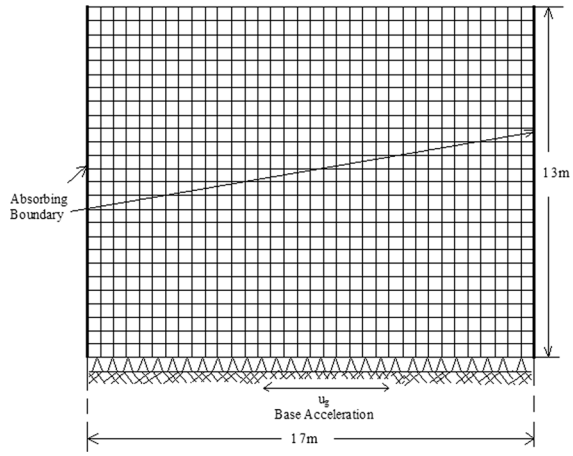

Fig. 13 Numerical discretization of soil domain in FLAC 2D

nonlinear curves are then fitted with multiple points using "*sigmoidal*" model available in FLAC (Itasca 2005). The "*sigmoidal*" curves are monotonic within the defined range, and have the appropriate asymptotic behavior, hence these functions are well suited for the purpose of representing modulus degradation curves. The "*sigmoidal*" model in FLAC 2D is defined as follows:

$$M_s = \frac{a}{1 + \exp\left(\frac{-(L - x_o)}{b}\right)} \tag{3}$$

where, L is the logarithmic strain, $L = \log_{10}(\gamma)$, a, b and x_o are the curve fitting parameters whose values for the Kasai River sand are 1.014, −0.525 and −2.650, respectively. Figure 9 shows the test data and the fitted curves utilized in the numerical analyses for the hysteretic damping and the modulus degradation of the Kasai River sand.

The excess pore water pressures developed in the test and that predicted by the numerical analysis are shown at 0.31 and 0.52 m depths in Fig. 14a, b. The numerical analysis predicts the liquefaction of the sand a little bit earlier than that observed in the model test. In both, model test and numerical analysis, the liquefaction initiates at a shallow depth (at 0.31 m) first, but the excess pore water pressure is found to fluctuate with the sinusoidal loadings. This fluctuation in the pore water pressure is not prominent in the test results due to the limited number of data points. The experimentally determined pore water pressures were measured at time interval of 1.0 s, below which it could not be recorded. But the numerical analyses are

done at a much smaller time step (2.56×10^{-5} s). At a greater depth (at 0.52 m), though the liquefaction initiates later, the excess pore water pressure is not fluctuating significantly as in the shallower depth. The delay in the initiation of the liquefaction in the model test as compared to that found in the numerical analyses might be due to the proximity of the finite boundaries. From Fig. 14b, the mean stress is 3.1 kPa at which the soil liquefies, and it intersects the experimental curve at 3.6 s (7 cycles approx). The numerical curve intersects the mean stress at 3 s (6 cycles approx). The number of cycles to liquefaction of the sand is also estimated from the effective stress-time history at 0.30 and 0.50 m depths, and from observing at which instance effective stress is close to zero. Figure 15a, b show the effective stress-time history at the two foresaid points in the sand bed. From Fig. 15, it is observed that the soil liquefies at around 2.5–3.0 s for 0.3 m depth and at 3.0–3.5 s at a depth of 0.5 m, respectively. This implies that the soil at a shallower depth liquefies earlier as compared to soil at a deeper location. Thus the zone of liquefaction spreads downward from the top, a similar observation made by Florin and Ivanov (2006). From the characteristic liquefaction curve given in Fig. 4, the number of cycles is estimated to be around 8, for the corresponding cyclic deviator stress of 46 kPa [obtained from the numerical analysis done using GEOSTUDIO (QUAKE/W 2004)]. This number is very close to the number of cycles to liquefaction obtained from the shake table test and the numerical analysis. Table 5 shows the number of cycles needed for the liquefaction of the Kasai River sand by different methods. It may be concluded that the whole

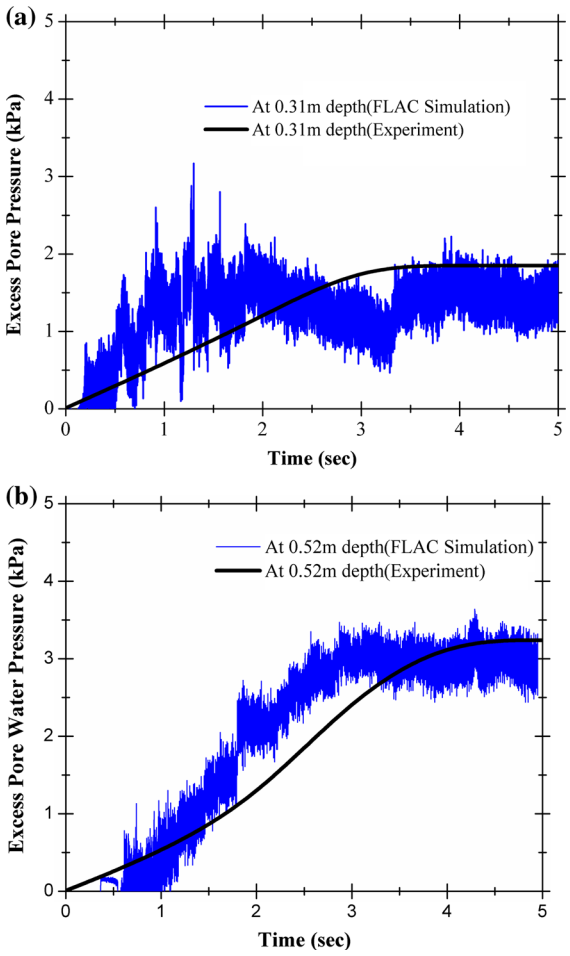

Fig. 14 Numerical validation of excess pore water pressure at **a** 0.31 m depth and **b** 0.52 m depth in Kasai river sand during liquefaction

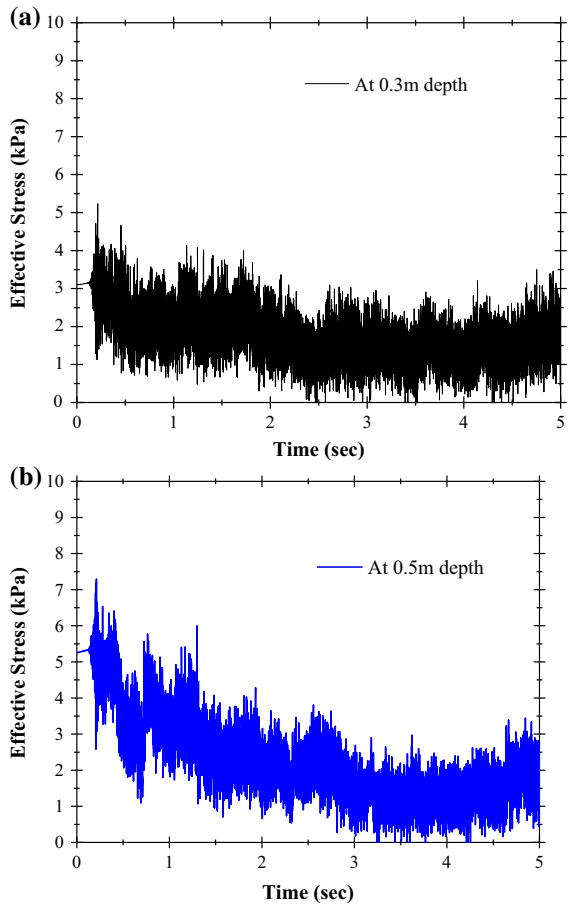

Fig. 15 Effective stress time history at **a** 0.3 m and **b** 0.5 m depths in Kasai River sand during liquefaction

Table 5 Number of load cycles required for liquefaction in different methods

Method	Number of cycles to liquefaction
Experiment	6.0–8.0
Numerical analysis (FLAC 2D)	6.0–7.0
Characteristics liquefaction curve	8.0
Cyclic triaxial test	8.0

soil liquefies around 6–8 cycles of assumed cyclic loading.

10 Conclusions

The engineering behavior of the dry and the saturated Kasai River sand at 67% relative density is studied experimentally on a shake table and numerically by FLAC2D when subjected to 10 sinusoidal cycles of amplitude 0.35 g at 2 Hz frequency. The cyclic triaxial data, shake table tests as well as the numerical analyses show coherently that the Kasai River sand liquefies in about 8 cycles of 0.35 g sinusoidal motion at 2 Hz. It is found that the maximum settlement in the dry sand deposit during shaking is around 10 mm. The maximum settlement increases to 26 mm after liquefaction under the same loading condition. Significant volume changes occur (around 4%) when there is liquefaction and followed by densification of the sand. In case of the dry sand, the volumetric strain is around 1.53% which is comparatively much less. As the dry sand offers more stiffness than in its liquefied state, the amplification of PGA at the ground level is much higher (around 1.9 times) in the liquefied sand than in the dry sand. The maximum value of lateral spreading at the surface in case of the liquefied sand is also significantly higher (about 2.50 times) as compared to that in the dry sand. This indicates that a much higher degree of damage may be expected for superstructures if the Kasai River sand liquefies.

Acknowledgements The authors sincerely acknowledge the financial support provided by SERB, Department of Science and Technology, India for this research work.

References

ASTM standard D5311 (2011) Test method for load controlled cyclic triaxial strength of soil. Annual book of ASTM standards, ASTM International West Conhohocken PA

Bandyopadhyay S, Sengupta A, Reddy GR (2015) Performance of sand and shredded rubber tire mixture as a natural base isolator for earthquake protection. Earthq Eng Eng Vib 14(4):683–693

Bhatia SC, Kumar MR, Gupta HK (1999) A probabilistic seismic hazard map of India and adjoining regions. Ann Di Geofis 42(6):1153–1164

Bhattacharya S, Lombardi D, Dihoru L, Dietz M, Crewe AJ, Taylor CA (2011) Model container design for soil-structure interaction studies. Role Seism Test Facil Perform Based Earthq Eng Springer Ser Geotech Geol Earthq Eng 22:135–158

Bryne PM (1991) A model for predicting liquefaction induced displacement. In: Proceedings, 2nd International Conference on Recent Advances in Geotechnical Earthquake Engineering and Soil Dynamics, St. Louis, Missouri 2:1027–1035

Castro G (1975) Liquefaction and cyclic mobility of saturated sands. J Geotech Eng Div 101(6):551–569

Castro G, Poulos SJ (1977) Factors affecting liquefaction and cyclic mobility. J Geotech Eng Div 103(6):501–516

Coe CJ, Prevost JH, Scanlan RH (1985) Boundary effects in dynamic centrifuge model tests. Proc Cetrifuge Boulder 91:441–448

Dasgupta S, Narula PL, Acharyya SK, Banerjee J (2000) Seismotectonic Atlas of India and its Environs. Geological Society of India, Kolkata, India

Dash SR (2010) Lateral pile—soil interaction in liquefiable soils. Ph.D. Thesis, University of Oxford, UK

De Alba P, Chan CK, Seed HB (1975) Determination of Soil Liquefaction characteristics by Large-Scale Laboratory Test. Report NO.EERC 75-14, Earthquake Engineering Research Center, University of California, Berkeley: California

Dobry R, Taboada V, Liu L (1995) Centrifuge modeling of liquefaction effects during earthquakes. In: Proceedings of the 1st International Conference on Earthquake Geotechnical Engineering 3:1291–1324

Ecemis N (2013) Simulation of seismic liquefaction: 1-g model testing system and shaking table tests. Eur J Environ Civil Eng 17(10):899–919

Elgamal A, Yang Z, Adalier K, Sharp MK (2003) Effect of Rigid Container Size on Dynamic Earth Dam Response in Centrifuge Experiments.In: Proceedings of the 16th ASCE Engineering Mechanics Conference, July 16–18, University of Washington, Seattle, WA

Florin VA, Ivanov PL (2006) Liquefaction of saturated sandy soils. In: Proceedings of the 5th International Conference on Soil Mechanics and Foundation Engineering, Paris 1:107–111

Giri D, Sengupta A (2010) Dynamic behavior of small-scale model of nailed steep slopes. Geomech Geoeng Int J 5(2):99–108

Ha IS, Olson SM, Seo MW, Kim MM (2011) Evaluation of reliquefaction resistance using shaking table tests. Soil Dyn Earthq Eng 31(4):682–691

Hushmand B, Scott RF, Crouse CB (1988) Centrifuge liquefaction tests in a laminar box. Geotechnique 38(2):253–262

Iai S (1989) Similitude for shaking table tests on soil-structure-fluid model in 1 g gravitational field. Soils Found 29(1):105–118

IS:1893 (2002) Indian standard criteria for earthquake resistant design of structures, Part 1-general provisions and buildings, Fifth Revision, Bureau of Indian Standard, New Delhi

Ishihara K, Tatsuoka F, Yasuda S (1975) Undrained deformation and liquefaction of sand under cyclic stresses. Soils Found 15(1):29–44

Itasca (2005) User's guide for FLAC version 5.0. Itasca India Consulting, Nagpur: India

Jaky J (1944) The coefficient of earth pressure at rest. J Soc Hung Archit Eng 7:355–358

Kokusho T (1999) Water film in liquefied sand and its effect on lateral spread. J Geotech Geoenviron Eng 125(10):817–826

Kreyszig E (2010) Advanced engineering mathematics. Wiley, Hoboken

Kumar SS, Dey A and Krishna AM (2015) Dynamic response of river bed sands using cyclic triaxial tests. In: Proceeding of the 5th Young Indian Geotechnical Engineers Conference (5IYGEC), Vadodara, India, 486–495

Lee KL, Seed HB (1967) Dynamic strength of anisotropically consolidated sand. J Soil Mech Found Div 93(5):169–190

Lombardi D, Bhattacharya S (2012) Shaking table tests on rigid soil container with absorbing boundaries. 15WCEE, Lisbon

Maheshwari BK, Singh HP, Saran S (2012) Effects of reinforcement on liquefaction resistance of solani sand. J Geotech Geoenviron Eng 13(7):831–840

Martin GR, Finn WDL, Seed HB (1975) Fundamentals of liquefaction under cyclic loading. J Geotech Geoenv Eng 101(5):423–438

Mohajeri M, Towhata I (2003) Shake table tests on residual deformation of sandy slopes due to cyclic loading. Soils Found 43(6):91–106

Mullins JP, Arulanandan K, Mitchell JK, Chan CK, Seed HB (1977) Effects of sample preparation on sand liquefaction. J Geotech Eng Div 10(2):91–108

Poulos SJ, Castro G, France JW (1985) Liquefaction evaluation procedure. J Geotech Eng Div 111(6):772–792

QUAKE/W (2004) An Engineering Methodology. Geo-Slope International, Calgary: Canada

Raj A, Nath SK, Thingbaijam KKS (2008) A note on the recent earthquakes in the Bengal basin. Current Sci 95(9):1127–1129

Ravaska O (2006) Effect of testing conditions on the shear strength parameters-a numerical study. In: Proceedings of the Sixth International Conference on Numerical Methods in Geotechnical Engineering Graz Austria 161–165

Sasaki Y, Towhata I, Tokida K, Yamada K, Matsumoto H, Tamari Y, Saya S (1992) Mechanism of permanent displacement of ground caused by seismic liquefaction. Soils Found 32(3):79–96

Seed HB (1979) Soil liquefaction and cyclic mobility evaluation for level ground during earthquakes. J Geotech Eng Div 105(2):201–255

Seed HB, Idriss IM (1971) A simplified procedure for evaluating soil liquefaction potential. J Soil Mech Found Div 97(9):1249–1274

Seed HB, Lee KL (1966) Liquefaction of saturated sands during cyclic loading. J Soil Mech Found Div 92:105–134

Seed HB, Martin PP, Lysmer J (1976) Pore-water pressure changes during soil liquefaction. J Geotech Eng Div 102(4):323–346

Seed HB, Tokimatsu K, Harder L, Chung R (1985) Influence of SPT procedures in soil liquefaction resistance evaluations. J Geotech Eng Div 111(12):1425–1445

Seed HB, Wong RT, Idriss IM, Tokimatsu K (1986) Moduli and damping factors for dynamic analysis of cohesionless soils. J Geotech Eng Div 112(11):1016–1032

Thevanayagam S, Kanagalingam T, Reinhorn A, Tharmendhira R, Dobry R, Pitman M, Abdoun T, Elgamal A, Zeghal M, Ecemis N, El Shamy U (2009) Laminar box system for 1 g physical modeling of liquefaction and lateral spreading. Geotech Test J 32(5):438–449

Towhata I, Sesov V, Motamed R (2006) Model Tests on Lateral Earth Pressure on Large Group Pile Exerted by Horizontal Displacementof Liquefied Sandy Ground. 8th U.S. National Conference on Earthquake Engineering and 100th Anniversary Earthquake Conference, San Francisco, California

Toyota H, Towhata I, Imamura S, Kudo K (2004) Shaking table tests on flow dynamics in liquefied slope. Soils Found 44(5):67–84

Ueng TS, Wu CW, Cheng HW, Chen CH (2010) Settlements of saturated clean sand deposits in shaking table tests. Soil Dyn Earthq Eng 30(1):50–60

Vaid YP, Chern JC (1983) Effect of static shear on resistance to liquefaction. Soils Found 23(1):47–60

Vaid YP, Finn WDL (1978) Static shear and liquefaction potential. J Geotech Eng Div 105(10):1233–1246

Vaid YP, Chern JC, Tumi H (1985) Confining pressure, grain angularity and liquefaction. J Geotech Eng 111(10):1229–1235

Xenaki VC, Athanasopoulos GA (2003) Liquefaction resistance of sand-mixtures: an experimental investigation of the effect of fines. Soil Dyn Earthq Eng 23:183–194

Ye B, Ye G, Ye W, Zhang F (2013) A pneumatic shaking table and its application to a liquefaction test on saturated sand. Nat Hazards 66(2):375–388